EPJ Web of Conferences **93**, 02009 (2015)
DOI: 10.1051/epjconf/20159302009

Experimental neutron capture data of ^{58}Ni from the CERN n_TOF facility

P. Žugec[1,a], M. Barbagallo[2], N. Colonna[2], D. Bosnar[1], S. Altstadt[3], J. Andrzejewski[4], L. Audouin[5], V. Bécares[6], F. Bečvář[7], F. Belloni[8], E. Berthoumieux[8,9], J. Billowes[10], V. Boccone[9], M. Brugger[9], M. Calviani[9], F. Calviño[11], D. Cano-Ott[6], C. Carrapiço[12], F. Cerutti[9], E. Chiaveri[8,9], M. Chin[9], G. Cortés[11], M.A. Cortés-Giraldo[13], M. Diakaki[14], C. Domingo-Pardo[15], R. Dressler[16], I. Duran[17], N. Dzysiuk[18], C. Eleftheriadis[19], A. Ferrari[9], K. Fraval[8], S. Ganesan[20], A.R. García[6], G. Giubrone[15], M.B. Gómez-Hornillos[11], I.F. Gonçalves[12], E. González-Romero[6], E. Griesmayer[21], C. Guerrero[9], F. Gunsing[8], P. Gurusamy[20], S. Heinitz[16], D.G. Jenkins[22], E. Jericha[21], Y. Kadi[9], F. Käppeler[23], D. Karadimos[14], N. Kivel[16], P. Koehler[24], M. Kokkoris[14], M. Krtička[7], J. Kroll[7], C. Langer[3], C. Lederer[3,25], H. Leeb[21], L.S. Leong[5], S. Lo Meo[26], R. Losito[9], A. Manousos[19], J. Marganiec[4], T. Martínez[6], C. Massimi[27], P.F. Mastinu[18], M. Mastromarco[2], M. Meaze[2], E. Mendoza[6], A. Mengoni[26], P.M. Milazzo[28], F. Mingrone[27], M. Mirea[29], W. Mondalaers[30], C. Paradela[17], A. Pavlik[25], J. Perkowski[4], M. Pignatari[31], A. Plompen[30], J. Praena[13], J.M. Quesada[13], T. Rauscher[31], R. Reifarth[3], A. Riegov[11], F. Roman[9,29], C. Rubbia[9,32], R. Sarmento[12], A. Saxena[20], P. Schillebeeckx[30], S. Schmidt[3], D. Schumann[16], G. Tagliente[2], J.L. Tain[15], D. Tarrío[17], L. Tassan-Got[5], A. Tsinganis[9], S. Valenta[7], G. Vannini[27], V. Variale[2], P. Vaz[12], A. Ventura[33], R. Versaci[9], M.J. Vermeulen[22], V. Vlachoudis[9], R. Vlastou[14], A. Wallner[25], T. Ware[10], M. Weigand[3], C. Weiß[21], and T. Wright[10]

[1] *Department of Physics, Faculty of Science, University of Zagreb, Croatia*
[2] *Istituto Nazionale di Fisica Nucleare, Bari, Italy*
[3] *Johann-Wolfgang-Goethe Universität, Frankfurt, Germany*
[4] *Uniwersytet Łódzki, Lodz, Poland*
[5] *Centre National de la Recherche Scientifique/IN2P3 - IPN, Orsay, France*
[6] *Centro de Investigaciones Energeticas Medioambientales y Tecnológicas (CIEMAT), Madrid, Spain*
[7] *Charles University, Prague, Czech Republic*
[8] *Commissariat à l'Énergie Atomique (CEA) Saclay - Irfu, Gif-sur-Yvette, France*
[9] *European Organization for Nuclear Research (CERN), Geneva, Switzerland*
[10] *University of Manchester, Oxford Road, Manchester, UK*
[11] *Universitat Politecnica de Catalunya, Barcelona, Spain*
[12] *Instituto Tecnológico e Nuclear, Instituto Superior Técnico, Universidade Técnica de Lisboa, Lisboa, Portugal*
[13] *Universidad de Sevilla, Spain*
[14] *National Technical University of Athens (NTUA), Greece*
[15] *Instituto de Física Corpuscular, CSIC-Universidad de Valencia, Spain*
[16] *Paul Scherrer Institut, Villigen PSI, Switzerland*
[17] *Universidade de Santiago de Compostela, Spain*
[18] *Istituto Nazionale di Fisica Nucleare, Laboratori Nazionali di Legnaro, Italy*
[19] *Aristotle University of Thessaloniki, Thessaloniki, Greece*
[20] *Bhabha Atomic Research Centre (BARC), Mumbai, India*
[21] *Atominstitut, Technische Universität Wien, Austria*
[22] *University of York, Heslington, York, UK*
[23] *Karlsruhe Institute of Technology, Campus Nord, Institut für Kernphysik, Karlsruhe, Germany*
[24] *Department of Physics, University of Oslo, N-0316 Oslo, Norway*
[25] *University of Vienna, Faculty of Physics, Austria*
[26] *Agenzia nazionale per le nuove tecnologie, l'energia e lo sviluppo economico sostenibile (ENEA), Bologna, Italy*
[27] *Dipartimento di Fisica e Astronomia, Università di Bologna, and Sezione INFN di Bologna, Italy*
[28] *Istituto Nazionale di Fisica Nucleare, Trieste, Italy*
[29] *Horia Hulubei National Institute of Physics and Nuclear Engineering - IFIN HH, Bucharest - Magurele, Romania*
[30] *European Commission JRC, Institute for Reference Materials and Measurements, Retieseweg 111, B-2440 Geel, Belgium*
[31] *Department of Physics and Astronomy - University of Basel, Basel, Switzerland*
[32] *Laboratori Nazionali del Gran Sasso dell'INFN, Assergi (AQ),Italy*
[33] *Istituto Nazionale di Fisica Nucleare, Bologna, Italy*

Abstract. The neutron capture cross section of ^{58}Ni was measured at the neutron time of flight facility n_TOF at CERN, from 27 meV to 400 keV neutron energy. Special care has been taken to identify all the possible sources of background, with the so-called neutron background obtained for the first time using high-precision GEANT4 simulations. The energy range up to 122 keV was treated as the resolved resonance region, where

51 resonances were identified and analyzed by a multilevel *R*-matrix code SAMMY. Above 122 keV the code SESH was used in analyzing the unresolved resonance region of the capture yield. Maxwellian averaged cross sections were calculated in the temperature range of kT = 5 – 100 keV, and their astrophysical implications were investigated.

1 Introduction

Neutron capture on ^{58}Ni is of importance for Nuclear Astrophysics, since ^{58}Ni is a participant in the slow neutron capture process (*s*-process) responsible for the production of a large portion of elements heavier than iron. It is also important as a constituent in the structural materials used in nuclear reactors, since the long lived ^{59}Ni – produced by the neutron irradiation of ^{58}Ni – is a source of the long-term radiation hazard. Furthermore, the subsequent ^{59}Ni$(n,\alpha)^{56}$Fe reaction contributes to the helium production within the stainless steel alloys, damaging them in the process [1].

2 n_TOF facility and experimental setup

At the neutron time of flight facility n_TOF at CERN the highly intense neutron beam is produced through irradiation of the massive Pb spallation target by 20 GeV pulsed proton beam from CERN Proton Synchrotron. The 7 ns wide proton pulses are delivered with a repetition rate in multiples of 1.2 s, with an average frequency of 0.4 Hz. Around 300 neutrons are produced per incident proton, with an average value of 7×10^{12} protons per pulse. Initially fast neutrons are moderated by the Pb block itself, 1 cm layer of water from the target cooling system and an additional 4 cm layer of borated water. After moderation the neutron beam covers 12 orders of magnitude in energy – from ∼10 meV to ∼10 GeV. An evacuated beamline leads to the experimental area located at approximately 185 m from the spallation target. Charged particles are deflected outside the neutron beam by a 1.5 T sweeping magnet. Further details on the n_TOF facility may be found in Ref. [2].

For the measurement of the ^{58}Ni(n,γ) reaction two C_6D_6 (deuterated benzene) liquid scintillation detectors were used, specifically optimized to exhibit a very low neutron sensitivity [3]. The measurement was performed by detecting the prompt γ-rays from the deexcitation cascades following the neutron captures. Based on the timestamp of a detected γ-ray – relative to the initial γ-flash preceding every neutron bunch – a kinetic energy is assigned to the captured neutron via the time of flight technique.

The mass of ^{58}Ni sample – 0.72 mm thick and 19.9 mm in diameter – was 2.069 g. The isotopic enrichment was 99.5%, with only trace contamination of ^{60,61,62,64}Ni.

3 ^{58}Ni neutron capture cross section

Neutron capture data were analyzed between 27 meV and 400 keV [4]. From the measured counts the capture yield was reconstructed applying the Pulse Height Weighting Technique [5], which consists in the off-line software modification of the detection efficiency so as to make it proportional to the total energy released in the cascade. Special care was taken to account for all possible sources of background. The background of scattered in-beam γ-rays was measured with the Pb sample and was found to be completely negligible. The background related to the neutron beam alone was measured without the sample in place. The environmental background – caused by the natural and induced radioactivity – was measured by turning off the neutron beam. Finally, the background caused by the neutrons scattered off the sample itself – referred to as the *neutron background* – was determined for the first time at n_TOF by dedicated GEANT4 [6] simulations. In the simulations a realistic description of the experimental hall and setup was implemented, and the details of the neutron interactions were recorded. Special care was taken in selecting the optimal set of models for the neutron transport and in investigating the reliability of simulated results. By comparing the simulated and experimental results for ^{nat}C sample – serving as an excellent neutron scatterer – the reliability of simulations was established [7]. The simulated neutron background for ^{58}Ni was subtracted from the experimental data in order to obtain the final capture yield, shown in Fig. 1.

The energy region up to 122 keV was analyzed as a resolved resonance region, where 51 resolved resonances were identified and analyzed by a multilevel *R*-matrix code SAMMY [8]. In fitting the resonances in the capture yield, SAMMY is able to account for the experimental effects such as the resolution function of the neutron beam, Doppler broadening, multiple scattering and self shielding effects, reconstructing the underlying capture cross section parameters in the process. Two resonances at nega-

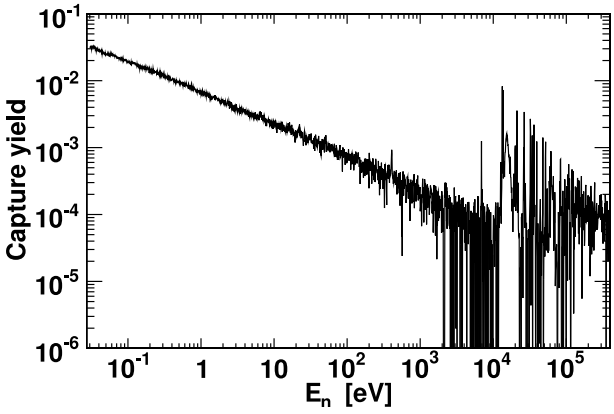

Figure 1. Capture yield of ^{58}Ni, corrected for all types of background.

[a]e-mail: pzugec@phy.hr

tive energies (below the neutron separation energy) were also adopted in order to parameterize the smooth capture yield extending from thermal energies up to the first capture resonance at 6.9 keV. The energy region from 122 keV to 400 keV was treated as the unresolved resonance region. In this region the specialized code SESH [9] was used to simulate the smoothed capture yield and thus reconstruct the smooth capture cross section. The parameterization from SESH was used to estimate the cross section all the way up to 1 MeV.

From the set of parameters obtained by SAMMY and SESH the Maxwellian averaged cross sections (MACS):

$$\langle\sigma\rangle_{kT} = \frac{2}{\sqrt{\pi}} \cdot \frac{1}{(kT)^2} \int_0^\infty \sigma(E_n) E_n e^{-E_n/kT} \mathrm{d}E_n \quad (1)$$

were calculated for the astrophysically relevant thermal values of kT = 5 – 100 keV, characteristic of the stellar environments where the *s*-process takes place. The latest n_TOF results are shown in Fig. 2, together with the past experimental results from Refs. [10–13] and the values adopted in the KADoNIS v0.3 database [14]. The recent findings by Guber et al. [13] – consisting in globally lower capture cross section than previously reported – are strongly supported by the latest n_TOF results. This may very well be due to the inadequately suppressed or subtracted neutron background in earlier experiments. In fact, a clear historical trend of lowering the reported MACS for ^{58}Ni may be observed. The MACS from n_TOF were also compared with the values calculated using the evaluated capture cross sections from ENDF/B-VII.0 [15] and ENDF/B-VII.1 [16] libraries, with ENDF/B-VII.0 capture data for ^{58}Ni as the representative of other major libraries such as JENDL-4.0, JEFF-3.1.2, CENDL-3.1 and ROSFOND-2010. Since the latest ENDF/B-VII.1 evaluation takes into account the results from Guber et al., above kT = 10 keV the n_TOF MACS were found to be in a better agreement with the MACS from ENDF/B-VII.1 than with those from ENDF/B-VII.0. Therefore, the revision of the evaluated capture data for ^{58}Ni is strongly encouraged for the other evaluated cross section libraries.

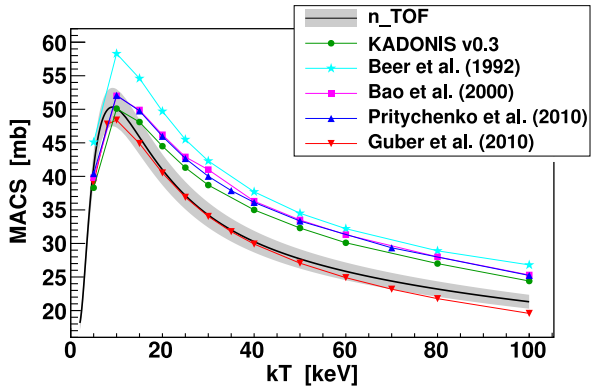

Figure 2. MACS from n_TOF – with an associated uncertainty range – compared to the past experimental results from Refs. [10–13] and values from KADoNIS v0.3 database [14].

The astrophysical implications of the n_TOF MACS were investigated by means of the post-processing NuGrid code MPPNP [17]. The new MACS value of 34.2 mb at kT = 30 keV – as opposed to 38.7 mb from the latest KADoNIS v0.3 database [14] – was used in the full 25M$_\odot$ stellar model with initial metal content of Z = 0.02. It was found that ^{58}Ni is efficiently depleted by the *s*-process in both cases, regardless of the MACS value used. For this reason the abundances of heavier isotopes along the *s*-process path leading from ^{58}Ni are not affected. However, due to 12% decrease in the average capture cross section – relative to KADoNIS v0.3 value – the small residual final ^{58}Ni content at the end of *s*-process is increased by 60% [4].

References

[1] V. Gopalakrishnan et al., J. Nucl. Materials **228**, 207 (1996)
[2] C. Guerrero et al., Eur. Phys. J. A **49**, 27 (2013)
[3] R. Plag et. al., Nucl. Inst. Meth. A **496**, 425 (2003)
[4] P. Žugec et al., Phys. Rev. C 8**9,** 014605 (2014)
[5] R. L. Macklin and J. H. Gibbons, Phys. Rev. **159**, 1007 (1967)
[6] S. Agostinelli et al., Nucl. Inst. Meth. A **506**, 250 (2003)
[7] P. Žugec et al., Nucl. Inst. Meth. A **760**, 57 (2014)
[8] N. M. Larson, Oak-Ridge National Laboratory Technical Report No. ORNL/TM-9179/R8 (2008)
[9] F. Froehner, SESH code, Gulf General Atomic Report No. GA-8380 (1968)
[10] H. Beer et al., Astrophys. J. Suppl. Ser. **80**, 403 (1992)
[11] Z. Y. Bao et al., At. Data Nucl. Data Tables **76**, 70 (2000)
[12] B. Pritychenko et al., At. Data Nucl. Data Tables **96**, 645 (2010)
[13] K. H. Guber et al., Phys. Rev. C **82**, 057601 (2010)
[14] I. Dillmann et al., AIP Conf. Proc. **819**, 123 (2006)
[15] M. B. Chadwick et al., Nucl. Data Sheets **107**, 2931 (2006)
[16] M. B. Chadwick et al., Nucl. Data Sheets **112**, 2887 (2011)
[17] F. Herwig et al., PoS (NIC X) 023 (2008)